



ESFANDIAR NAVA-YAZDANI, HANS-CHRISTIAN HEGE¹,
CHRISTOPH VON TYCOWICZ², TIM SULLIVAN

A Shape Trajectories Approach to Longitudinal Statistical Analysis

¹  0000-0002-6574-0988

²  0000-0002-1447-4069

Zuse Institute Berlin
Takustr. 7
14195 Berlin
Germany

Telephone: +49 30-84185-0
Telefax: +49 30-84185-125

E-mail: bibliothek@zib.de
URL: <http://www.zib.de>

ZIB-Report (Print) ISSN 1438-0064
ZIB-Report (Internet) ISSN 2192-7782

A Shape Trajectories Approach to Longitudinal Statistical Analysis

Esfandiar Nava-Yazdani Hans-Christian Hege¹
Christoph von Tycowicz² Tim Sullivan

July 31, 2018

Abstract


For Kendall's shape space we determine analytically Jacobi fields and parallel transport, and compute geodesic regression. Using the derived expressions, we can fully leverage the geometry via Riemannian optimization and reduce the computational expense by several orders of magnitude. The methodology is demonstrated by performing a longitudinal statistical analysis of epidemiological shape data.


As application example we have chosen 3D shapes of knee bones, reconstructed from image data of the Osteoarthritis Initiative. Comparing subject groups with incident and developing osteoarthritis versus normal controls, we find clear differences in the temporal development of femur shapes. This paves the way for early prediction of incident knee osteoarthritis, using geometry data only.

1 Introduction

In recent years, there has been an increased interest in statistical analysis of geometric shapes. Especially in the field of morphometry such analyses are performed - but mostly for static forms. A frequently encountered situation, however, is that instead of a set of discrete shapes, series of shapes are given, often together with co-varying parameters. A particular example are longitudinal imaging studies, tracking biological shape changes over time within and across individuals to gain insight into dynamical processes like aging or disease progression. For better understanding of such temporal shape data, statistical modeling and analysis of shapes is of critical importance.

The main challenge is that shape variability is inherently nonlinear and high-dimensional, so that classical statistical approaches are not always appropriate. One way to address this is linearization. The quality of the resulting statistical model, however, then depends strongly on the validity of the linearity assumption, i.e. that the observed data points lie to a good approximation in a flat Euclidean subspace. Since the natural variability in populations often leads to a large spread in shape space and the observed data may lie in highly-curved regions (see [HH14]), linearity can often not be assumed in practical applications.

¹  0000-0002-6574-0988

²  0000-0002-1447-4069

In the context of longitudinal studies, an important task is to estimate continuous trajectories from sparse and potentially noisy samples. For smooth individual biological changes, subject-specific spatiotemporal regression models are adequate. They provide also a way to describe the data at unobserved times (i.e. shape changes between observation times and - within certain limits - also at future times) and to compare trends across subjects in the presence of unbalanced data (e.g. due to drop outs). An approach used is to approximate the observed temporal shape data by geodesics in shape space and based on these, estimate overall trends within groups. Geodesic models are attractive as they feature a compact representation (similar to the slope and intercept term in linear regression) and therefore allow for computationally efficient inference.

The intrinsic theory of least squares and geodesic regression has been introduced by Fletcher in [Fle13]. Derivation of the corresponding Euler-Lagrange equations for some important manifolds can be found in the work of Machado and Leite [ML07]. For an overview of statistical analysis on Riemannian manifolds see the work of Huckemann and Hotz [HH14] and Pennec [Pen06].

An additional challenge in the analysis of shape trajectories is to distinguish between morphological differences due to (i) temporal shape evolutions of a single individual and (ii) the geometric variability in a population of an object class under study. To obtain a statistically significant localization of structural changes at the population level (group-wise statistics), the subject-specific trajectories need to be transferred in a standard reference frame. Among the different techniques proposed for normalizing longitudinal deformations [RCSO⁺04, BZO10], constructions based on *parallel transport* provide the most natural approach and have shown superior sensitivity and stability in the context of diffeomorphic registration [LAP11]. Note also that for general trajectories, the simple transport of each shape is not suitable because the distances between the shapes are not preserved. But if the shapes belong to the same geodesic, this problem does not arise. This is another advantage of geodesic regression.

As parallel transport in curved shape spaces is rarely given in closed form, in general it has to be approximated numerically, e.g. employing Schild's ladder. For Kendall's shape space, most computations, including parallel transport, can be reduced to those for the pre-shape sphere, so that via horizontal projections closed form expressions are possible. For shapes in 2D, Kendall's shape space is isomorphic to the projective space, which is a symmetric space, so that the essential geometric quantities are well known (cf. [HHM10] and [Fle13]). But for three and more dimensions, because of less restrictive structure, many questions remain open.

The paper is organized as follows: In Section 2, we provide an overview of Kendall's shape space. For the determination of the canonical decomposition of tangent vectors of the pre-shape space in horizontal and vertical components, which is essential for the geometry and analysis of shapes and trajectories, we provide a computationally efficient approach via the so-called Sylvester equation. Moreover, we use this decomposition to determine parallel transport and Jacobi fields, which will be employed for geodesic regression. Parallel transport is significant in statistical normalization, alignment of trajectories and also computation of Jacobi fields.

The latter describes the variability of trajectories that will be modeled as best fitting geodesics in Section 3. There, we present our algorithm for the computation of geodesic regression. In Section 4 we apply this to longitudinal

statistical analysis of femur data from an epidemiological study dealing with osteoarthritis and discuss the numerical results.

2 Geodesic Analysis in Shape Space

A pre-shape is a k -ad of landmarks (i.e. particular points) in \mathbb{R}^m after removing translations and similarity transformations. A shape is a pre-shape with rotations removed. For a comprehensive introduction to Kendall's shape space and details on the subjects of this section, we refer to [KBCL99].

2.1 Shape Space

In the following we present some preliminaries on Kendall's shape space, provide a computationally efficient method to determine horizontal and vertical components of tangent vectors of the pre-shape space, and also prove the corresponding SO_m -equivariance.

Let $M(m, k)$ denote the space of real $m \times k$ matrices. In order to remove translations, we replace $x \in M(m, k)$ by $x - \bar{x}$ where \bar{x} denotes the Euclidean mean of x_1, \dots, x_k . The result $R_m^k := \{x \in M(m, k) : \sum_{i=1}^k x_i = 0\}$ identified with $M(m, k-1)$ will be endowed with its canonical scalar product given by $\langle x, y \rangle = \text{trace}(xy^t)$. Denoting the Frobenius norm by $\|\cdot\|$, we call the sphere $\mathcal{S}_m^k := \{x \in R_m^k : \|x\| = 1\}$ pre-shape space and endow it with the spherical Procrustes metric $d(x, y) = \arccos(\langle x, y \rangle)$. Now, the left action of SO_m on \mathcal{S}_m^k , $(R, x) \mapsto Rx$ defines an equivalence relation given by $x \sim y$ iff $y = Rx$ for some $R \in SO_m$. Kendall's shape space is defined as $\Sigma_m^k = \mathcal{S}_m^k / \sim$. Provided that $k \geq m+1$, the dimension of Σ_m^k is $m(k-1) - \frac{1}{2}m(m-1) - 1$. Now, denoting the canonical projection of \sim by π , the induced distance between any two shapes $\pi(x)$ and $\pi(y)$ is given by

$$d_\Sigma(x, y) = \min_{R \in SO_m} d(x, Ry) = \arccos \sum_{i=1}^m \lambda_i$$

where $\lambda_1 \geq \dots \geq |\lambda_m|$ denote the pseudo-singular values of yx^t . Denoting $\mathcal{D}_j := \{x \in \mathcal{S}_m^k : \text{rank}(x) \leq j\}$, it turns out that $\Sigma_{m,m}^k := \Sigma_m^k \setminus \pi(\mathcal{D}_{m-2})$ inherits a differential structure, compatible with its quotient topology. Following [KBCL99], we refer to $\pi(\mathcal{D}_{m-2})$ as the singular part of Σ_m^k . In particular, Σ_m^k is a strata of manifolds with varying dimensions and $\Sigma_{m,m}^k$ is open and dense in Σ_m^k . Away from the singular part, the quotient map π is a Riemannian submersion. Moreover, for $k \geq 3$ the shape spaces Σ_1^k and Σ_2^k are isometric to sphere resp. projective space. For each $x, y \in \mathcal{S}_m^k$ there exists a rotation $R \in SO_m$ such that Ryx^t is symmetric and $d(x, Ry) = d_\Sigma(x, y)$. We say that R well positions y to x and $\tilde{y} := Ry$ is well positioned to x . Note that R does not need to be unique. Let U denote a neighbourhood in \mathcal{S}_m^k with radius smaller than $\pi/4$ (diameter of Σ_m^k is $\pi/2$) such that

$$\lambda_{m-1} + \lambda_m > 0 \text{ for all } x, y \in U.$$

Obviously, U is invariant under the action of SO_m . For $x, y \in U$ the optimal rotation R and hence \tilde{y} are unique and the function

$$\mathcal{S}_m^k \ni y \mapsto \omega(x, y) := \tilde{y}$$

is well-defined. Well-positionedness is symmetric, i.e. $y = \omega(x, y)$ implies $x = \omega(y, x)$. If x and y are well positioned, we write $x \overset{\omega}{\sim} y$. For $x \overset{\omega}{\sim} y$ the horizontal geodesic from x to y is given by

$$\Phi(t, x, y) := \exp_x(t \log_x y) = \frac{\sin((1-t)\varphi)}{\sin \varphi} x + \frac{\sin(t\varphi)}{\sin \varphi} y \quad (1)$$

where $\varphi = \arccos(\langle x, y \rangle)$, $0 \leq t \leq 1$, \exp and \log denote the exponential and logarithm in the pre-shape space. Hence Φ realizes the minimizing geodesic from $\pi(x)$ to $\pi(y)$. We recall that the vertical space at $x \in \mathcal{S}_m^k$ is given by

$$Ver_x = \{Ax : A + A^t = 0\}$$

and the horizontal space by

$$Hor_x = \{u \in M(m, k-1) : ux^t = xu^t \text{ and } \text{trace}(xu^t) = 0\}.$$

Hence the restriction of $d_x \pi$ to Hor_x is an isometry of Euclidean vector spaces Hor_x and $T_{\pi(x)} \Sigma_m^k$. We denote the vector space of $m \times m$ skew-symmetric real matrices by $Skew_m$. Thus $Ver_x = Skew_m \cdot x$. As appropriate for our applications and for brevity, unless otherwise specified, we restrict our data to the open and dense set of full rank pre-shapes $S := \{x \in \mathcal{S}_m^k : \text{rank}(x) = m\}$. As π is a Riemannian submersion, the geometry of the shape space is mainly described by its horizontal lift in the pre-shape space.

Lemma 2.1. *Let $x \in S$ and ver_x denote the restriction of vertical projection to $T_x \mathcal{S}_m^k$. Then the following hold.*

a) $\text{ver}_x(w) = Ax$ where A is the solution of the Sylvester equation

$$Axx^t + xx^t A = wx^t - xw^t.$$

b) Fix $R \in SO_m$. Then $\text{ver}_{Rx}(Rw) = R\text{ver}_x(w)$.

Proof. S is open in \mathcal{S}_m^k . Hence $T_x S = T_x \mathcal{S}_m^k$. Now, the claims follow from a straightforward computation utilizing that A is unique (since xx^t and $-xx^t$ have no eigenvalues in common) and skew-symmetric (since right hand side is skew-symmetric). For b) note that $\langle Rw, Rx \rangle = \langle w, x \rangle = 0$, i.e., $w \in T_x S$ implies $Rw \in T_{Rx} S$. Now, $\text{ver}_{Rx}(Rw) = BRx$ where B is the solution of $BRxx^t + xx^t R^t B = R(wx^t - xw^t)R^t$. Hence $B = RAR^t$ implying $\text{ver}_{Rx}(Rw) = R.\text{ver}_x(w)$. \square

Henceforth superscripts v and h denote the vertical resp. horizontal component, i.e., for any $w \in T_x \mathcal{S}_m^k$ we have $w = \langle w, x \rangle x + w^h + w^v$ where the decomposition is orthogonal. Due to the explicit computation above, $(R.w)^v = R.w^v$ and $(R.w)^h = R.w^h$, i.e., horizontal and vertical projections are SO_m -equivariant. Denoting the covariant derivatives in the pre-shape and shape space by ∇ resp. $\tilde{\nabla}$, for horizontal vector fields X and Y we have

$$(\tilde{\nabla}_{d\pi X} d\pi Y) \circ \pi = d\pi(\nabla_X Y).$$

In the following $[\cdot, \cdot]$ denotes the Lie bracket in $M(m, k-1)$, i.e., $[U, V] = DV(U) - DU(V)$ (D Euclidean). For the Euclidean derivative of a vector field

W along a curve γ we use $\frac{D}{dt}$ and also for simplicity of notation a dot, i.e., $\nabla_{\dot{\gamma}}W = \dot{W} - \langle \dot{W}, \dot{\gamma} \rangle \gamma$ if $\|\dot{\gamma}\| = 1$, and $\frac{D^2W}{dt^2} = \ddot{W}$, etc. We set¹

$$\text{Log}_x y := \log_x \omega(x, y), \text{Exp}_x u := \exp_x u^h, u \in T_x \mathcal{S}_m^k.$$

For the computation of the Fréchet mean (cf. [HHM10] and [Pen06]) \bar{p} of the shapes $p_1, \dots, p_N \in U$, i.e.,

$$\bar{p} := \arg \min G, G(x) = \sum_{i=1}^N d_{\Sigma}^2(x, p_i) \quad (2)$$

we apply Newton's method to Karcher's equation $\sum_{i=1}^N \text{Log}_x p_i = 0$ as follows. We search for the unique zero \bar{p} of the function f defined by

$$f(x) = \sum_{i=1}^N \text{Log}_x p_i, x \in U$$

and set

$$x_{k+1} = \text{Exp}_{x_k}(-(d_{x_k} f)^{-1} f(x_k)).$$

A suitable initial value is the normalized Euclidean mean

$$x_0 = \frac{1}{\|\sum_{i=1}^N p_i\|} \sum_{i=1}^N p_i.$$

The total variance of $p = (p_1, \dots, p_N)$ reads

$$\text{var}(p) = \frac{1}{N} G(\bar{p}) = \frac{1}{N} \sum_{i=1}^N \|\text{Log}_{\bar{p}} p_i\|^2.$$

2.2 Parallel Transport

Next, we consider parallel transport in the shape space and its relation to parallel transport in the pre-shape space². We call a vector field W along a horizontal curve γ horizontally parallel (for brevity h-parallel) iff W is horizontal and $d\pi W$ is parallel along $\pi \circ \gamma$.

Proposition 2.1. *Let γ be a horizontal curve in S , u a horizontal vector at $x := \gamma(0)$ and W a vector field along γ with $W(0) = u$. Then the following holds.*

a) *The vector field W is h-parallel transport of $d\pi u$ if and only if w satisfies*

$$\dot{W} = A\gamma - \langle W, \dot{\gamma} \rangle \gamma, A\gamma\gamma^t + \gamma\gamma^t A = \dot{\gamma}W^t - W\dot{\gamma}^t. \quad (3)$$

b) *Suppose that γ is a unit speed geodesic. Then the equations (3) reduce to*

$$\dot{W} = A\gamma - \langle W, \dot{\gamma} \rangle \gamma, \dot{A}\gamma\gamma^t + \gamma\gamma^t \dot{A} + 3(A\dot{\gamma}\gamma^t + \gamma\dot{\gamma}^t A) = 0. \quad (4)$$

¹Note that the Riemannian exponential map of the shape space denoted by $\widetilde{\text{exp}}$ satisfies $\pi(\text{exp}_x u) = \widetilde{\text{exp}}_{\pi(x)}(d_x \pi(u)) = \widetilde{\text{exp}}_{\pi(x)}(d_x \pi(u^h))$.

²Essentially part a) of proposition 2.1 was recently also obtained by Kim, Dryden and Le (cf. [KDL18]).

c) Let W^S denote the parallel transport W^S of u along γ in the pre-shape space. Then $W = W^S$ if and only if vu^t is symmetric. In this case, if γ is a geodesic, then

$$W = U - 2 \frac{\langle u, y \rangle}{\|x + y\|^2} (x + y)$$

where U is the Euclidean parallel extension of u along γ and $y = \exp_x(v)$.

Proof. a) W is parallel if and only if $d\pi(\nabla_{\dot{\gamma}}W) = 0$, i.e., infinitesimal variation of W must be vertical. Hence $\nabla_{\dot{\gamma}}W = (\nabla_{\dot{\gamma}}W)^v$, which due to lemma 2.1 equals $A\gamma$ with $A\gamma\dot{\gamma}^t + \gamma\dot{\gamma}^t A = (\nabla_{\dot{\gamma}}W)\dot{\gamma}^t - \gamma(\nabla_{\dot{\gamma}}W)^t = \dot{W}\dot{\gamma}^t - \gamma\dot{W}^t$. Moreover, SO_m -equivariance of vertical projection implies the well-definedness, i.e., if $d\pi W$ is parallel, then $d\pi(Rw)$ is parallel for all $R \in SO_m$. Now, W is horizontal if and only if $\dot{f} = 0$ where $f := \|W\dot{\gamma}^t - \gamma\dot{W}^t\|^2 + \langle W, \dot{\gamma} \rangle^2$, since $f(0) = 0$. If the equations (3) hold, then $\dot{W}\dot{\gamma}^t - \gamma\dot{W}^t = (\nabla_{\dot{\gamma}}W)\dot{\gamma}^t - \gamma(\nabla_{\dot{\gamma}}W)^t = A\gamma\dot{\gamma}^t + \gamma\dot{\gamma}^t A = \dot{\gamma}W^t - W\dot{\gamma}^t$ and $\langle \dot{W}, \dot{\gamma} \rangle + \langle W, \dot{\gamma} \rangle = \langle A\gamma - \langle W, \dot{\gamma} \rangle \gamma, \dot{\gamma} \rangle + \langle W, \dot{\gamma} \rangle = \langle A\gamma, \dot{\gamma} \rangle = 0$. Hence $\dot{f} = 0$, i.e., W remains horizontal. If W is horizontal, then $\dot{f} = 0$ and we arrive at $A\gamma\dot{\gamma}^t + \gamma\dot{\gamma}^t A = \dot{\gamma}W^t - W\dot{\gamma}^t$. Thus (3) follows.

b) Note that $W\dot{\gamma}^t$ and $\dot{\gamma}W^t$ are symmetric and $\ddot{\gamma} + \gamma = 0$. Now, (3) implies

$$\begin{aligned} \dot{A}\dot{\gamma}^t + \gamma\dot{\gamma}^t \dot{A} + 2(A\dot{\gamma}^t + \gamma\dot{\gamma}^t A) &= \ddot{\gamma}W^t - W\ddot{\gamma}^t + \dot{\gamma}\dot{W}^t - \dot{W}\dot{\gamma}^t \\ &= \dot{\gamma}(A\gamma - \langle W, \dot{\gamma} \rangle \gamma)^t - (A\gamma - \langle W, \dot{\gamma} \rangle \gamma)\dot{\gamma}^t \\ &= -(A\gamma\dot{\gamma}^t + \dot{\gamma}\dot{\gamma}^t A). \end{aligned}$$

c) Obviously, $W = W^S$ if and only if $A = 0$, which is equivalent to $uv^t = vu^t$. For a unit speed geodesic

$$W^S = U + \langle u, v \rangle (\dot{\gamma} - v)$$

and a straightforward computation yields

$$W^S = U - 2 \frac{\langle u, y \rangle}{\|x + y\|^2} (x + y).$$

□

Note that the differential equation for the parallel transport can also be written as

$$(\nabla_{\dot{\gamma}}W)\dot{\gamma}^t\gamma\dot{\gamma}^t + \gamma\dot{\gamma}^t(\nabla_{\dot{\gamma}}W)\dot{\gamma}^t = (\dot{\gamma}W^t - W\dot{\gamma}^t)\gamma\dot{\gamma}^t. \quad (5)$$

Hence, a vector field along a curve in $\pi(S)$ is parallel, if and only if it has a horizontal lift satisfying the above equation.

2.3 Jacobi Fields

A smooth horizontal curve γ in \mathcal{S}_m^k is a geodesic if and only if $\pi \circ \gamma$ is a geodesic in Σ_m^k . Hence any geodesic variation of $\pi \circ \gamma$ in the latter space reads $\pi \circ H$ with H a variation of γ through horizontal geodesic. Hence the variation field $\frac{d}{ds}(\pi \circ H(s, \cdot))|_{s=0} = d\pi(\frac{d}{ds}H(s, \cdot)|_{s=0})$ is a Jacobi field of the shape space. In the following we derive the differential equation and present the solution for horizontal variation fields. Recall that a vector field J along γ is called normal iff $\langle J, \dot{\gamma} \rangle = 0$.

Theorem 2.1. *Let γ be a horizontal geodesic in S and J a horizontal vector field on S along γ . Then the following holds.*

a) $d\pi(J)$ is a Jacobi field if and only if

$$J + \left(\frac{D^2 J}{dt^2} \right)^h = 4 \left(\frac{D}{dt} \left(\frac{DJ}{dt} \right)^v \right)^h. \quad (6)$$

b) J is normal solution of (6) if and only if

$$J = \alpha U + \beta W$$

with $\alpha + \ddot{\alpha} = 0$, $4\beta + \ddot{\beta} = 0$, U and W h -parallel, $\dot{U} = 0$ and $\ddot{W} + W = 0$

c) Suppose that γ is unit speed. Then any normal solution J of (6) can be expressed as

$$J = \cos_1 U_1 + \cos_2 W_1 + \sin_1 U_2 + \frac{1}{2} \sin_2 W_2.$$

Here $\sin_n(t) := \sin(nt)$, $\cos_n(t) := \cos(nt)$, w_n denotes the orthogonal projection of ξ_n to $\text{Skew}_m \cdot \dot{\gamma}$ and u_n its orthogonal complement, W_n and U_n parallel extensions of w_n resp. u_n and $\xi_1 = J(0)$, $\xi_2 = \dot{J}(0)$.

d) A Jacobi field J^S of the pre-shape sphere satisfies (6) if and only if

$$\left(\frac{D}{dt} \left(\frac{DJ^S}{dt} \right)^v \right)^h = 0$$

Proof. a) Obviously, any solution of the equation (6) is horizontal and due to SO_m -equivariance of horizontal and vertical projection, invariant under SO_m action. Now, fix a horizontal vector field Y along γ and let $X := \dot{\gamma}$. Denoting the Riemannian curvature of the shape space by \tilde{R} , due to O'Neill's formula (cf. [GHL05])

$$\langle \tilde{R}(d\pi J, d\pi X)d\pi X, d\pi Y \rangle = \langle J, X \rangle \langle X, Y \rangle - \langle X, X \rangle \langle J, Y \rangle + \frac{3}{4} \langle [J, X]^v, [X, Y]^v \rangle$$

The normal component of a Jacobi field is also a Jacobi field. Hence we may and do assume that $\langle X, J \rangle = 0$. Moreover, we may and do assume that γ is unit speed. Thus with $2(\nabla_X Y)^v = [X, Y]^v$ we have

$$\begin{aligned} \langle \tilde{R}(d\pi J, d\pi X)d\pi X, d\pi Y \rangle &= \frac{3}{2} \langle [J, X]^v, \nabla_X Y \rangle - \langle J, Y \rangle \\ &= \frac{3}{2} X \cdot \langle [J, X]^v, Y \rangle - \frac{3}{2} \langle \nabla_X [J, X]^v, Y \rangle - \langle J, Y \rangle \\ &= \langle \frac{3}{2} \nabla_X [X, J]^v - J, Y \rangle \\ &= \langle 3 \nabla_X (\nabla_X J)^v - J, Y \rangle. \end{aligned}$$

Now, $d\pi J$ is a Jacobi field if and only if $\tilde{R}(d\pi J, d\pi X)d\pi X = \tilde{\nabla}_{d\pi X}^2(d\pi J)$. Hence

$$\tilde{R}(d\pi J, d\pi X)d\pi X = \tilde{\nabla}_{d\pi X}(d\pi(\nabla_X J)) = d\pi(\nabla_X(\nabla_X J)^h).$$

Hence $\langle d\pi(\nabla_X(\nabla_X J)^h), d\pi Y \rangle = \langle 3 \nabla_X(\nabla_X J)^v - J, Y \rangle$, i.e.,

$$\langle \nabla_X(\nabla_X J)^h, Y \rangle = \langle 3 \nabla_X(\nabla_X J)^v - J, Y \rangle$$

which is equivalent to

$$J + (\nabla_X(\nabla_X J)^h)^h = 3(\nabla_X(\nabla_X J)^v)^h$$

and with $(\nabla_X J)^h = \nabla_X J - (\nabla_X J)^v$ we arrive at (6).

b) We may and do assume that γ is unit speed. Inserting δZ with Z horizontal and \dot{Z} vertical, in (6) yields

$$(\delta + \dot{\delta})Z = 3\delta\ddot{Z}^h.$$

A straightforward computation shows that αU and βW solve the above equation. To prove the converse suppose that γ is unit speed, let Cv be the tangent component of $Z(0)$ in $Skew_m \cdot v$ and u its orthogonal complement. By orthogonality u and Cv extend to parallel fields U and $W = C\dot{\gamma}$ along γ with $\dot{U} = 0$, $\ddot{W} + W = 0$ and we arrive at the desired decomposition. c) follows immediately from b). For d) note that $\frac{D^2 J^S}{dt^2} + J^S = 0$. \square

3 Geodesic Regression

In the following, we employ the results of the previous section to derive an efficient and robust approach for finding the relation between an independent scalar variable, i.e. time, and a dependent shape-valued random variable.

Regression analysis is a fundamental tool for the spatiotemporal modeling of longitudinal observations. Given scalars $t_1 < t_2 < \dots < t_N$ and distinct pre-shapes q_1, \dots, q_N , the goal of geodesic regression is to find a geodesic curve in shape space that best fits the data in a least-squares sense. In particular, let γ in \mathcal{S}_m^k be a horizontal geodesic, we define the sum-of-squared error of the data to the geodesic as

$$F(\gamma) := \sum_{i=1}^N d_{\Sigma}^2(q_i, \gamma(t_i)). \quad (7)$$

While in [Fle13] and [ML07] geodesics are identified with their initial point and velocity, hence consider $F(x, v)$ with $x = \gamma(0)$ and $v = \dot{\gamma}(0)$, we use the identification of γ with its endpoints, i.e., we consider

$$F(x, y) = \sum_{i=1}^N d_{\Sigma}^2(q_i, \gamma(t_i)) = \sum_{i=1}^N d_{\Sigma}^2(q_i, \Phi(t_i, x, y)), \quad x \overset{\omega}{\sim} y,$$

since computations of geodesics via Slerp (given by the function Φ defined in equation (1)) are more efficient. Model estimation is then formulated as the least-squares problem

$$(x^*, y^*) = \arg \min_{(x, y)} F(x, y).$$

In the absence of an analytic solution, the regression problem has to be solved numerically. To this end, we employ a Riemannian trust-regions solver [BMAS14] with an Hessian approximation based on finite differences and initial guess (q_1, q_N) . Having in mind that (cf. [Pen06] and [Jos17])

$$\nabla \rho_y(x) = -2\text{Log}_x y, \quad \text{Hess}(\rho_y)(x) = 2(D\text{Exp}_x(\text{Log}_x y))^{-1} D_x \text{Exp}_x(\text{Log}_x y)$$

where $\rho_y(x) := d_{\Sigma}^2(x, y)$, both the gradient and Hessian of the cost function F can be computed utilizing the Jacobi fields, since the derivatives of the exponential map and therefore those of Φ are given by the Jacobi fields.

4 Application to Epidemiological Data

In this section, we analyze the morphological variability in longitudinal data of distal femora in order to quantify shape changes that are associated with femoral osteoarthritis.

We apply the derived scheme to the analysis of group differences in longitudinal femur shapes of subjects with incident and developing osteoarthritis (OA) versus normal controls. The dataset is derived from the Osteoarthritis Initiative (OAI), which is a longitudinal study of knee osteoarthritis maintaining (among others) clinical evaluation data and radiological images from 4,796 men and women of age 45-79. The data are available for public access at <http://www.oai.ucsf.edu/>.

From the OAI database, we determined three groups of shapes trajectories: HH (healthy, i.e. no OA), HD (healthy to diseased, i.e. onset and progression to severe OA), and DD (diseased, i.e. OA at baseline) according to the Kellgren–Lawrence score [KL57] of grade 0 for all visits, an increase of at least 3 grades over the course of the study, and grade 3 or 4 for all visits, respectively. We extracted surfaces of the distal femora from the respective 3D weDESS MR images (0.37×0.37 mm matrix, 0.7 mm slice thickness) using a state-of-the-art automatic segmentation approach [ATEZ18]. For each group, we collected 22 trajectories (all available data for group DD minus a record that exhibited inconsistencies, and the same number for groups HD and HH, randomly selected), each of which comprises shapes of all acquired MR images, i.e. at baseline, the 12-, 24-, 36-, 48- and 72-month visits. In a supervised post-process, the quality of segmentations as well as the correspondence of the resulting meshes (8,988 vertices) were ensured.

We apply the geodesic regression approach detailed in Section 3 to the femoral shape trajectories described above and represented in Kendall’s shape space. The resulting estimated geodesics along with the original trajectories are visualized in Fig. 1. Due to the expressions derived for the parallel transport and Jacobi fields, we can fully leverage the geometry using Riemannian optimization procedures. In particular, we observed a superlinear convergence of the intrinsic trust-region solver in most cases. Solving the high-dimensional (53,928 degrees of freedom) regression problem on a laptop computer with Intel Core i7-7500U (2 × 2.70GHz) CPU took about 0.3 seconds in average. In contrast, generic nonlinear Matlab routines required about 25 seconds to determine a solution, thus being two orders of magnitude slower.

Next we would like to answer the question of how well the observed data is replicated by the estimated geodesic trends. A common approach to test this is to compute the *coefficient of determination*, denoted as R^2 , that is the proportion of the total variance in the data explained by the model. Following [Fle13], a generalization to manifolds is defined as

$$R^2 = 1 - \frac{\text{unexplained variance}}{\text{total variance}} = 1 - \frac{\min_{\gamma} F(\gamma)}{\min_x G(x)},$$

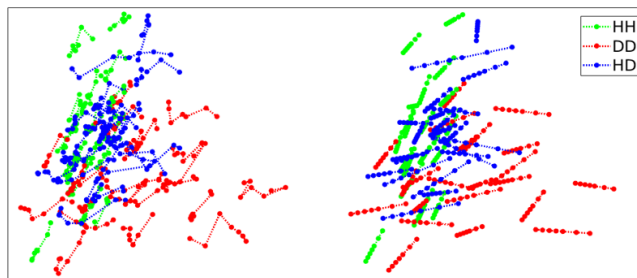


Figure 1: First two principal coefficients for femoral shape trajectories of subjects with no (HH), progressing (HD), and severe (DD) osteoarthritis (left) and their qualitatively estimated shape trajectories via geodesic regression (right). The figure indicates that regression provides a plausible model. Significant difference in cross-group trends is observed. Note that on the left side, the data points are the original shapes, while on the right side these are their projections to the respective regression geodesic.

with $F(\gamma)$ and $G(x)$ as defined in equations (7) and (2), respectively. As the unexplained variance cannot exceed the total variance (since the Fréchet mean lies in the search space of the regression problem) and both variances are non-negative, R^2 must lie in the interval $[0, 1]$ – with larger values indicating a higher proportion of the variance being explained by the model.

The coefficients of determination were computed for all estimated trends amounting to average group-wise R^2 values of 0.38, 0.54, and 0.51 for group HH, DD, and HD, respectively. While for all groups the geodesic model is able to describe a relatively large portion of the shape variability, there is a *clear difference* between the control group HH and the groups DD and HD associated to osteoarthritis. In particular, pairwise Mann–Whitney U tests confirm that the differences are highly unlikely due to random chance (with p -values of 0.000, and 0.005 for HH vs. DD, and HH vs. HD, respectively). These findings indicate that the OA related shape changes are well captured by a single variable (time), whereas the physiological effects in HH are rather related to multiple explanatory variables.

Based on the coefficient of determination we also test for the significance of the estimated trends employing permutation tests as suggested in [Fle13]. For each of the trajectories we performed 1,000 permutations and considered the results as statistically significant for p -values less than 0.01. In almost all cases (63 out of 66) the trends were significant, such that we can expect them to be highly unlikely due to random chance.

As shown in Fig. 2 we also observed clear differences in cross-group trends of mean trajectories. This result in particular indicates that computing mean of the geodesics for each group in the tangent bundle is very appropriate. Indeed, the mentioned means of geodesics provide (as described in [MF12]) group parameters (intercept and slope) and can be employed for analysis of disease growth and prediction.

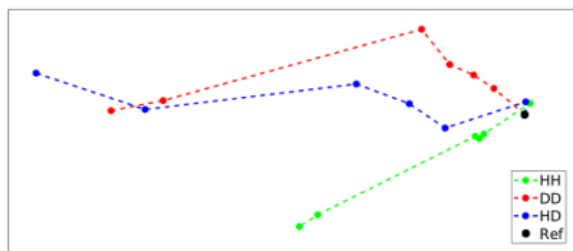


Figure 2: First two principal coefficients of aligned mean trajectories after alignment via parallel transport to the reference (mean of baseline shapes in HH).

Furthermore, we computed the lengths of trajectories and shape wise distances. As expected, diseased groups provided a higher variability. In particular, computation of the trajectory lengths provided min., mean and max. values 0.0438, 0.0665 and 0.0968 for HH, 0.0512, 0.0691 and 0.0992 for DD and 0.0566, 0.0784 and 0.1091 for HD. Also, average distances of mean shapes to shapes in the reference trajectory (mean of the healthy group) visualized in Fig. 3 proved to be articulately higher for HD.

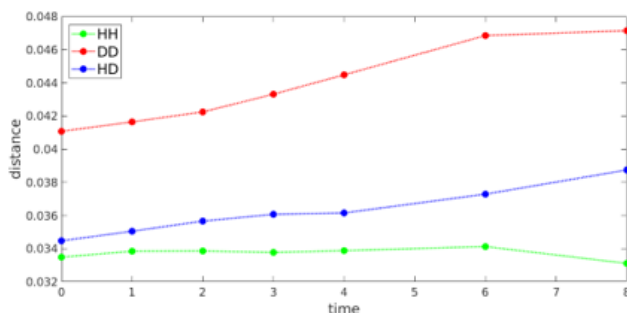


Figure 3: Average distance of the mean shapes to shapes in the reference trajectory for all time points.

5 Concluding Remarks

This work presented characterizations and computationally efficient methods for determination of parallel transport, Jacobi fields and geodesic regression of data represented as shapes in Kendall's space. Furthermore, an application to longitudinal statistical analysis of epidemiological data (femur data for analysis of knee osteoarthritis) has been shown.

An advantage of modeling trajectories by geodesics is the following: A main task in the longitudinal analysis is to translate trajectories to start at a reference shape. The intermediate distances between the shapes of a geodesic are preserved by parallel transport, while they are not for general trajectories.

Moreover, data inconsistencies are minimized by considering the best-fitting geodesics, and Jacobi fields can be employed to analyze the variability of the geodesics, hence providing a canonical descriptor of trends and differences for the trajectories. There are many potential avenues for future work: First, group-wise means of the geodesics in each group can be computed with respect to a natural metric in the tangent bundle (e.g. the Sasaki metric) to determine the group parameters for a mixed-effects model as described in [MF12]. Second, an extension of the method to higher-dimensional longitudinal parameters instead of just time can be examined, to achieve even more differentiated results. Third, a natural generalization is provided by spline regression. Finally, the methodology can be employed for maximum likelihood estimation (cf. [Fle13]) and utilized for outlier detection.

On the application side, based on the results found, it can be said in summary that the shape trajectories of the three groups have characteristic progressions. It seems possible to make a correct assignment to one of the three groups based on just two measurements. The aim of further analyses must be to substantiate this statement, by answering the following question: With what reliability can a prediction be made about the onset of knee osteoarthritis – depending on the initial shape of the femur and the time interval between the first two image acquisitions?

Acknowledgements

This work was supported by the ECMath project CH 15 *Analysis of Empirical Shape Trajectories* (E. Nava-Yazdani) and DFG project *In-vivo soft tissue kinematics from dynamic MRI* (C. von Tycowicz). Furthermore we are grateful for the open-access dataset provided by OAI³ as well as for the open-source software Manopt [BMAS14].

References

- [ATEZ18] Felix Ambellan, Alexander Tack, Moritz Ehlke, and Stefan Zachow. Automated segmentation of knee bone and cartilage combining statistical shape knowledge and convolutional neural networks: Data from the Osteoarthritis Initiative. In *Medical Imaging with Deep Learning*, 2018.
- [BMAS14] Nicolas Boumal, Bamdev Mishra, P.-A. Absil, and Rodolphe Sepulchre. Manopt, a Matlab toolbox for optimization on manifolds. *Journal of Machine Learning Research*, 15:1455–1459, 2014.

³The Osteoarthritis Initiative is a public-private partnership comprised of five contracts (N01-AR-2-2258; N01-AR-2-2259; N01-AR-2-2260; N01-AR-2-2261; N01-AR-2-2262) funded by the National Institutes of Health, a branch of the Department of Health and Human Services, and conducted by the OAI Study Investigators. Private funding partners include Merck Research Laboratories; Novartis Pharmaceuticals Corporation, GlaxoSmithKline; and Pfizer, Inc. Private sector funding for the OAI is managed by the Foundation for the National Institutes of Health. This manuscript was prepared using an OAI public use data set and does not necessarily reflect the opinions or views of the OAI investigators, the NIH, or the private funding partners.

- [BZO10] Matias Nicolas Bossa, Ernesto Zacur, and Salvador Olmos. On changing coordinate systems for longitudinal tensor-based morphometry. In *Spatiotemporal Image Analysis for Longitudinal and Time-Series Image Data*, 2010. CD publication.
- [Fle13] P. Thomas Fletcher. Geodesic regression and the theory of least squares on Riemannian manifolds. *International Journal of Computer Vision*, 105(2):171–185, 2013.
- [GHL05] Sylvestre Gallot, Dominique Hulin, and Jacques Lafontaine. *Riemannian Geometry*. Springer, 2005. (3rd ed., pages 151 ff.).
- [HH14] Stephan Huckemann and Thomas Hotz. On means and their asymptotics: circles and shape spaces. *Journal of Mathematical Imaging and Vision*, 50(1-2):98–106, 2014.
- [HHM10] Stephan Huckemann, Thomas Hotz, and Axel Munk. Intrinsic shape analysis: Geodesic PCA for Riemannian manifolds modulo isometric Lie group actions. *Statistica Sinica*, 20(1):1–58, 2010.
- [Jos17] Jürgen Jost. *Riemannian Geometry and Geometric Analysis*. Springer, 2017. (7th ed., pages 251 ff.).
- [KBCL99] David George Kendall, Dennis Barden, Thomas K Carne, and Huiling Le. *Shape and Shape Theory*. John Wiley & Sons, 1999.
- [KDL18] Kwang-Rae Kim, Ian L Dryden, and Huiling Le. Smoothing splines on Riemannian manifolds, with applications to 3d shape space. *arXiv preprint arXiv:1801.04978*, 2018.
- [KL57] JH Kellgren and JS Lawrence. Radiological assessment of osteoarthritis. *Annals of the Rheumatic Diseases*, 16(4):494, 1957.
- [LAP11] Marco Lorenzi, Nicholas Ayache, and Xavier Pennec. *Schild’s Ladder for the Parallel Transport of Deformations in Time Series of Images*, pages 463–474. Springer Berlin Heidelberg, 2011.
- [MF12] Prasanna Muralidharan and P. Thomas Fletcher. Sasaki metrics for analysis of longitudinal data on manifolds. In *2012 IEEE Conference on Computer Vision and Pattern Recognition, Providence, RI, USA, June 16-21, 2012*, pages 1027–1034, 2012.
- [ML07] Luís Miguel Machado and F Silva Leite. Fitting smooth paths on Riemannian manifolds. *International Journal of Applied Mathematics and Statistics*, 4(J06):25–53, 2007.
- [Pen06] Xavier Pennec. Intrinsic statistics on Riemannian manifolds: Basic tools for geometric measurements. *Journal of Mathematical Imaging and Vision*, 25(1):127, 2006.
- [RCSO⁺04] A. Rao, R. Chandrashekar, G.I. Sanchez-Ortiz, R. Mohiaddin, P. Aljabar, J.V. Hajnal, B.K. Puri, and D. Rueckert. Spatial transformation of motion and deformation fields using nonrigid registration. *IEEE Transactions on Medical Imaging*, 23(9):1065–1076, 2004.